Click to view slide presentation

[EA]Insights from Geomechanical Modelling of 2D Cross-Sections in Fold-Thrust Belts*

Reinaldo Ollarves[1], Samuel Fraser[1], and Ken McClay[2]

Search and Discovery Article #30672 (2020)**
Posted September 7, 2020

*Adapted from extended abstract prepared in conjunction with oral presentation given at 2020 Asia Pacific Region, AAPG/EAGE 1st Petroleum Geoscience Conference & Exhibition, PNG's Oil and Gas Industry Maturing through Exploration, Development and Production, Port Moresby, Papua New Guinea, 25-27 February 2020
 DOI:10.1306/30672Ollarves2020

[1]Santos Limited, Adelaide, Australia (reinaldo.ollarves@santos.com)
[2]Australian School of Petroleum, Adelaide University, Adelaide, Australia

Abstract

A holistic approach for the validation of structural models of fold and thrust belts integrates geomechanical modelling into the balancing and restoration workflows. This approach enables testing forward numerical models incorporating variable mechanical stratigraphies and fault frameworks in order to understand the progressive evolution and final geometries of fold and thrust systems. The combined multi-component workflows improve interpretations and gives confidence in areas of poor seismic and no subsurface data.

Four forward mechanical models of simple inverted extensional faults are used to demonstrate the importance of mechanical stratigraphy in the development of thick and thin-skinned fold and thrust systems as well as demonstrating the application of forward modelling for section balancing in contractional terranes.

Introduction

Understanding the complex subsurface geometries of fold and thrust belts typically involves geometrical cross-section construction and restoration techniques in order to validate 2D seismic interpretations. Although these methods involve well-established geometric rules based on field and subsurface studies, they do not include any quantitative consideration of the elastic moduli and physical properties of the strata in the system.

Many fold and thrust belts include both thin skinned - i.e. detached above the rigid crystalline basement, and thick-skinned deformation - i.e. inversion of pre-existing basement involved rift fault systems whereby the basement is involved and uplifted. Well-documented examples of combined thick and thin-skinned fold and thrust belts include those of the Sub-Andean system in Venezuela, Colombia, Peru, Bolivia, and Argentina; in the Apennines; in the frontal sectors of the western Alps; in the French and Spanish Pyrenees, as well as in the foreland fold and

thrust belts of Papua New Guinea. Geomechanical tools, such as Dynel (Schlumberger) uses Finite Element Modelling (FEM) code to honour the fundamental physics that govern crustal deformation. Dynel also can simulate the behaviour of strata with inhomogeneous and anisotropic elastic properties (Maerten and Maerten, 2006).

This method allows analysis of:

(a) The strain distribution throughout the layered model as it deforms from both overburden induced lithostatic pressure and applied lateral compressive stresses;
(b) The different responses and interactions of stratal packages with different mechanical properties; and
(c) How mechanical stratigraphy controls the styles of faulting and folding that determine the structural evolution of fold and thrust belts.

Methodology

The evolution of four forward models of inverted listric faults was simulated using Dynel. The stress and strain distributions were simulated using the parameters outlined in Table 1.

Model 1 - the baseline model of an inverted simple listric growth fault with reactivation of the main listric fault and uniform post-rift stratigraphy (Figure 1a);
Model 2 - inversion of a simple listric fault as in Model 1 but with a mechanicially strong uppermost layer simulating a thick limestone package (Figure 1b);
Model 3 - inversion of a simple listric fault as in model 2 but with propagation of the main fault with a convex-upwards geometry into the post-rift strata (Figure 1c);
Model 4 - inversion of a simple listric fault as in model 2 but with a footwall shortcut fault that forms a frontal wedge structure (Figure 1d).

For each model incremental horizontal shortening was applied and the final geometries are summarised below in Figure 2. Incremental and total stress and strain distributions were calculated for each stage of deformation. The Dynel parameters used for the physical properties of the strata are shown in Table 1. All models experienced three equal stages of incremental contractional displacement along the main fault system in order to directly compare both the evolution and final deformation states between the models.

Discussion

Figure 2 summarises the incremental strains and displacement vector fields for the final deformation of each of the four models. In all models shortening produced reactivation of the main listric fault with the production of an asymmetric uplifted anticline with steeper frontal limbs and gently dipping back limbs (Figure 2). Strain and stress concentrations occurred along the steepest portions on the original listric fault system. In general the incremental displacement vectors in the hanging walls are parallel to sub-parallel to the trajectory of the main listric fault but near the steeper sections and fault tip, the displacement vectors become steeper and nearly vertical except for Model 4 where the development of a footwall short-cut underneath the steep section of the main listric fault induces lower angle displacement vectors sub-parallel to the short-cut (Figure 2d). All models show low deformation in the vicinity of the crestal collapse graben.

In addition, strain and stress concentrations commonly occur at the upper tips of the antithetic crestal collapse faults (e.g. Figure 2a and Figure 2b) as well at the upper-tips of the back-thrusts in Model 3 (Figure 2c). Maximum hanging occurs in models 2 and 3 wall uplift where there is competent limestone unit at the top of the model.

Greatest variations in hanging-wall architectures occur in models 3 and 4 where there are significant changes in the trajectory of the main inverted fault system. In Model 3 the propagation of the main listric fault along a convex-up ramp system into the anisotropic weak layers of the post-rift strata produced a thin-skinned flap with less steeply dipping displacement vectors (Figure 2c). In contrast the introduction of a footwall short-cut produced less uplift and a wider inversion anticline and a frontal wedge system (Figure 2d).

These simple geomechanical Dynel models illustrate how changes in mechanical stratigraphy and in fault trajectories strongly control the hanging-wall fold architectures, as well as strain and stress distributions. These features are not incorporated nor produced by purely geometric and kinematic models. Natural examples of inversion structures show many similar features to those developed in the Dynel models. These allow better prediction of structures at depth as well as realistic evolutionary models that indicate how complex subsurface structures may have formed. Detailed analysis of the numerical mechanical models may permit better fracture predictions both in basement systems as well as in supra-basement reservoirs where variations in mechanical stratigraphy may be crucial for reservoir characterisation.

Acknowledgements

We would like to express our gratitude to Laurent Maerten for his fruitful discussions about Dynel and the use of geomechanical models. We thank John Chambers for his support and encouragement. Schlumberger for providing constant software support. Last but not least to Santos Ltd for allowing this work to be presented.

References Cited

Butler, R.W.H., C.E. Bond, M.A. Cooper, and H. Watkins, 2018, Interpreting Structural Geometry in Fold-Thrust Belts: Why Style Matters: Journal of Structural Geology, v. 114, p. 251-273. doi.org/10.1016/j.jsg.2018.06.019

Maerten, L., and F. Maerten, 2006, Chronologic Modeling of Faulted and Fractured Reservoirs Using Geomechanically Based Restoration: Technique and Industry Applications: American Association of Petroleum Geologist Bulletin, v. 90/8, p. 1201-1226.

Wilkerson, M.S. and C. Dicken, 2001, Quick-Look Techniques for Evaluating Two-Dimensional Cross Sections in Detached Contractional: American Association of Petroleum Geologist Bulletin, v. 85/10, p. 1759-1770.

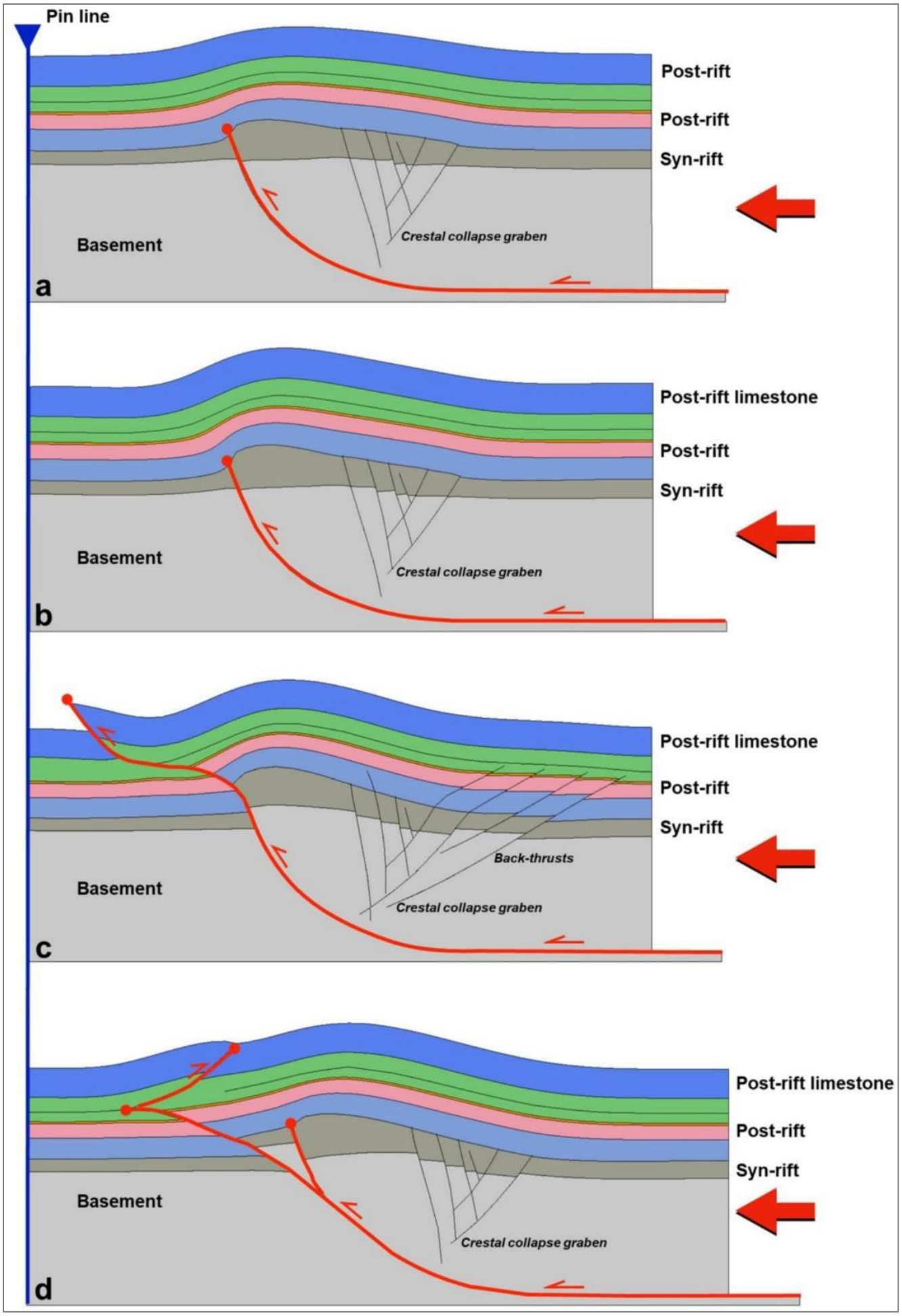

Figure 1. Final stage of deformation of four key inversion models. (a) Model 1. Baseline model of an inverted simple listric growth fault with reactivation of the main listric fault and uniform post-rift stratigraphy; (b) Model 2. Inversion of a simple listric fault as in Model 1 but with a mechanicially strong uppermost layer simulating a thick limestone package; (c) Model 3. Inversion of a simple listric fault as in model 2 but with propagation of the main fault with a convex-upwards geometry into the post-rift strata; and (d) Model 4. Inversion of a simple listric fault as in model 2 but with a footwall shortcut fault that forms a frontal wedge structure.

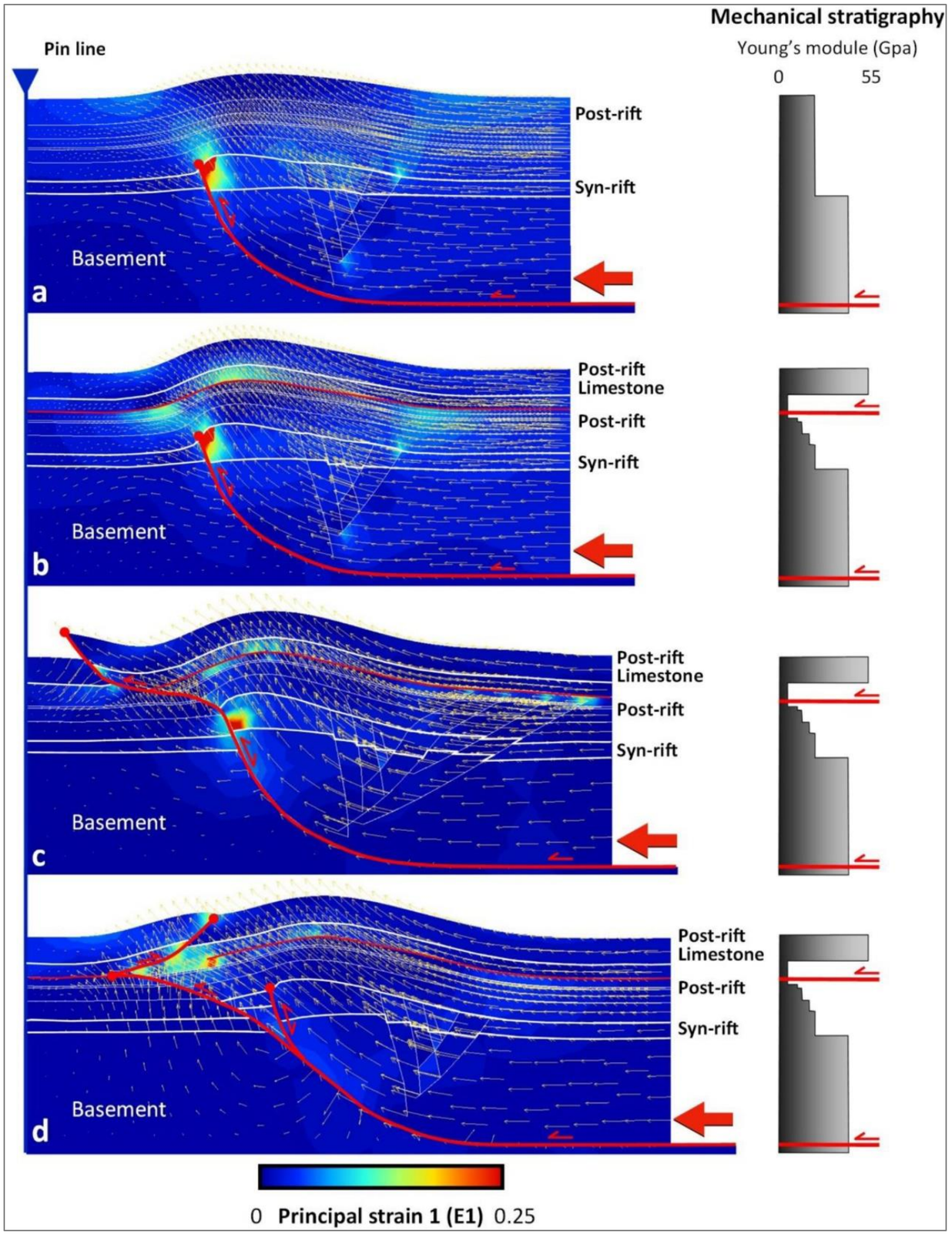

Figure 2. Final incremental principal strains 1 (E1) and displacement vectors -yellow arrows- (left side). Mechanical stratigraphy showing Young's Modulus and location of detachment layers (right side). (a) Model 1; (b) Model 2; (c) Model 3; and (d) Model 4.

Model	Basement lithology (Young's modulus (GPa))	Syn-rift strata (Young's modulus (GPa))	Post-rift strata (Young's modulus (Gpa))
1	Granite (45)	Sandstones (22)	Sandstones (22)
2	Granite (45)	Sandstones (22)	Sandstones with shales & limestones (4.8 – 55)
3	Granite (45)	Sandstones (22)	Sandstones with shales & limestones (4.8 – 55)
4	Granite (45)	Sandstones (22)	Sandstones with shales & limestones (4.8 – 55)

Table 1. Summary of model parameters.